Mat. Res. Soc. Symp. Proc. Vol. 703 © 2002 Materials Research Society V3.9

Dynamic Fracture Mechanisms in Nanostructured and Amorphous Silica Glasses Million-Atom Molecular Dynamics Simulations.

Laurent Van Brutzel, Cindy L. Rountree, Rajiv K. Kalia, Aiichiro Nakano, and Priya Vashishta
Concurrent Computing Laboratory for Materials Simulations,
Biological Computation and Visualization Center,
Department of Physics and Astronomy, Department of Computer Science, Louisiana State University, Baton Rouge, Louisiana 70803

ABSTRACT

Parallel molecular dynamics simulations are performed to investigate dynamic fracture in bulk and nanostructured silica glasses at room temperature and 1000 K. In bulk silica the crack front develops multiple branches and nanoscale pores open up ahead of the crack tip. Pores coalesce and then they merge with the advancing crack-front to cause cleavage fracture. The calculated fracture toughness is in good agreement with experiments. In nanostrucutred silica the crack-front meanders along intercluster boundaries, merging with nanoscale pores in these regions to cause intergranular fracture. The failure strain in nanostructured silica is significantly larger than in the bulk systems.

INTRODUCTION

Amorphous silica (a-SiO_2) is widely used in various technological applications because of its unique chemical and physical properties. However, the brittle nature and poor shock resistance of silica have precluded its use as a structural material. With the synthesis of "ductile" nanophase ceramics, there is renewed hope that novel amorphous nanostructured silica systems that fracture more gracefully than conventional bulk a-SiO_2 will find use in structural applications. However, any hope to enhance mechanical properties rests on understanding crack initiation and propagation at the atomic scale. Ten years ago Simmons and al. carried out the first Molecular Dynamics simulations to investigate brittle fracture in a-SiO_2 [1-3]. They showed that the crack in a-SiO_2 is not only initiated by the surface defects but also has an origin in the intrinsic structure. Nevertheless, these simulations were not large enough to study the propagation on a largest scale.

We present here results of Molecular Dynamics (MD) simulations on crack propagation and fracture in both bulk a-SiO_2 and nanostructured a-SiO_2 at low and high temperatures. These simulations, involving a million-atom each, are performed with reliable inter-atomic potentials on parallel computers using highly efficient algorithms. In the bulk system at room temperature (300 K), we find that the crack-front propagates by merging with the cavities that open up just ahead of it. In contrast, the bulk system at 1000 K many more cavities both close and far from the crack-tip appear. Those far from the crack-tip coalesce before merging with the main crack forming a secondary crack. In the nanostructured a-SiO_2 at room and high temperature, we observe intergranular fracture with the crack meandering along the nanoparticle boundaries. The observed crack propagation and fracture behavior in both bulk and nanostructured silica are related to the inherent intermediate range order in these systems.

COMPUTATIONAL PROCEDURE

MD simulations of silica are performed with a reliable inter-atomic potential, consisting of two-body and three-body terms [4]. The two-body terms contain the effects of charge transfer, electronic polarization, and steric repulsion. The three-body terms is a Stillinger-Weber like potential involving bond bending and bond stretching effects. The potential is validated through a detailed comparison with various experimental results on bulk silica glass such as elastic moduli, static structure factor, and phonon density of states [5, 6].

Fracture simulations in bulk and nanostructured silica glasses are performed on systems containing a million atoms each. The two bulk a-SiO_2 systems were prepared by melting β-cristobalite at 3500 K, thermalizing it for 30,000 time steps, before cooling it gradually to 3000 K where it was again thermalized for 30,000 time steps. Following this procedure of gradual cooling and thermalization, the system was cooling down to 5 K and then subjected to conjugate-gradient quench which brought down the temperature to 0 K. This system was then heated to 300 K where it was further thermalized for 50,000 time steps, subsequently, the temperature was raised to 1000 K and this system was also relaxed for 50,000 time steps.

The nanostructured system was prepared by cutting out spheres of radius 40 Å from the well thermalized bulk amorphous system [7]. These spherical nanoparticles were relaxed with the conjugate gradient technique. Subsequently, 100 of these nanoparticules were randomly placed in a box and consolidated at 1000 K with the application of a hydrostatic pressure that was gradually increased to 16 GPa. Keeping the pressure fixed, the system was cooled from 1000 K to 300 K and the system was relaxed for 30,000 time steps. Subsequently the pressure was slowly decreased to zero. This consolidated system at 0 GPa and 300 K has a density of 2.04 g/cc which is close to the bulk density (2.2 g/cc). The nanostructured glass at 1000 K was obtained by heating the room temperature system and subsequently thermalizing it for 30,000 time steps.

To simulate dynamic fracture the periodic boundary conditions are removed. A triangular notch of length 50 Å and width 40 Å is created on one edge of the simulation box by removing atoms. The pre-notched systems is then subjected to an external strain by displacing the atoms included in the top and the bottom layers of the simulation box. The width of these layers is approximately equal to a cut-off. The strained systems is subsequently relaxed under isothermal conditions before increasing the strain further. In all the systems studied we applied a strain rate of 0.01/ps.

RESULTS AND DISCUSSION

Figure 1 shows snapshots of notch and pores in bulk a-SiO_2 at 300 K for different values of strains. Pores were analyzed by dividing each system into voxels of size 4.5 Å and then identifying empty voxels with a common edge or corner. Figure 1(a) shows the initial notch. Figure 1(b) displays that in bulk a-SiO_2 at 300 K small pores open up directly ahead of the crack tip when the strain exceeds 3.4%. In a region approximately of 50 Å ahead of the crack tip, pores coalesce to form cavities of dimensions between 20 Å and 60 Å. With further increase in

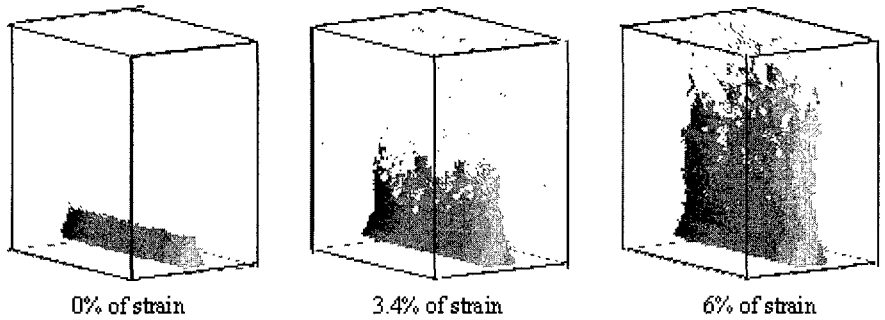

Figure 1. Snapshots of pores and cracks in bulk a-SiO_2 at 300 K. Fig. 1(a) shows the initial notch and fig. 1(b) and 1(c) show its evolution into several branches and the appearance of nanoscale pores at a strain of 3.4% and 6% respectively.

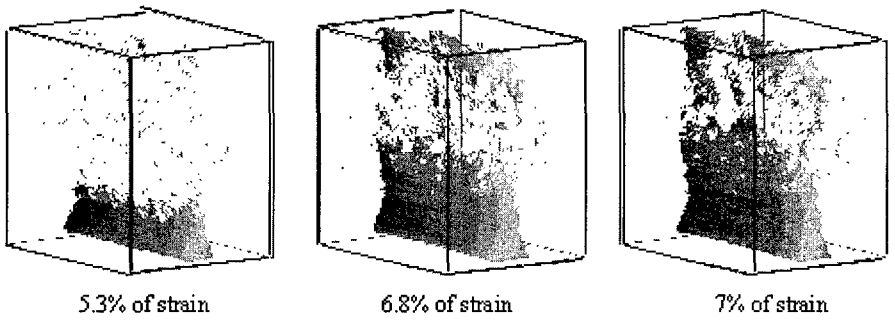

Figure 2. Snapshots of pores and cracks in bulk a-SiO_2 at 1000 K. The system at 1000 K shows little progression of the pre-notch even at a strain of 5.3% (fig. 2(a)). However in fig. 2(b), further increase in strain causes the crack-front to move significantly and in fig. 2(c) several cavities appear as a result of coalescence of nanoscale pores forming a distinct secondary crack.

the strain (Fig. 1(c)) the number of cavities increases and they form multiple branches on the crack-front. Finally, the system ruptures completely at a strain of 6.5 %.

Figure 2 shows many features of crack and pore evolution in a-SiO_2 at 1000 K similar to those observed at room temperature, the crack-front propagates by growth and coalescence of cavities. Nevertheless, the onset of crack in a-SiO_2 at 1000 K occurs at a strain of 5.3% whereas at room temperature it appears around 2%. Further analysis reveals that the glass at 1000 K has pores 100 Å ahead of the crack tip leading to the formation of a secondary crack, whereas in the room temperature system, pores are mostly combined closer to the crack tip.

Figures 3 show crack and pore evolution in nanostructured a-SiO_2 at 300 K. Small pores are formed in interfacial regions along nanoparticule boundaries even in the absence of the applied strain. As the strain increases pores grow, and some of them merge with the main crack while

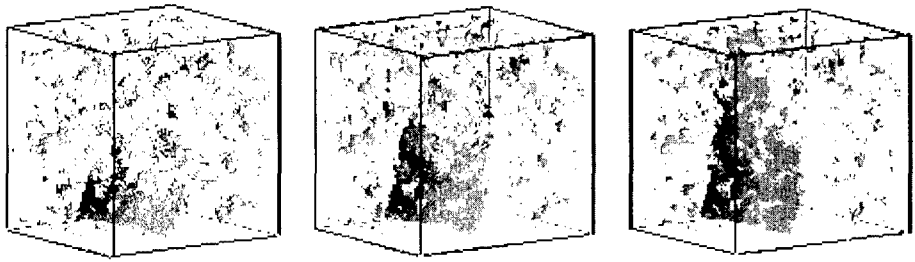

Figure 3. Snapshots of pores and cracks in nanostructured a-SiO_2 at 300 K. Fig. 3(a) displays the initial distribution of pores; in fig. 3(b) the pores show the interfacial regions between the clusters; and fig. 3(c) shows the evolution of the crack through the interfacial regions.

others coalesce to form a secondary cracks approximately 100 Å ahead the crack tip. At a strain of 9 %, the primary and secondary cracks merge to cause intergranular fracture.

Quantitatively, the similarities and differences between the three systems can be seen in Fig. 4(a) where the porosities are plotted as a function of the applied strain. The two bulk a-SiO_2 systems have nearly the same porosities up to a strain of 3.5%. With further increase in the strain, the porosity rises more sharply in the room temperature glass than in the system at 1000 K. In order to characterize more precisely the correlation between the number of pores and crack propagation the strain dependence of crack tip positions is also analyzed. In figure 4(b) the

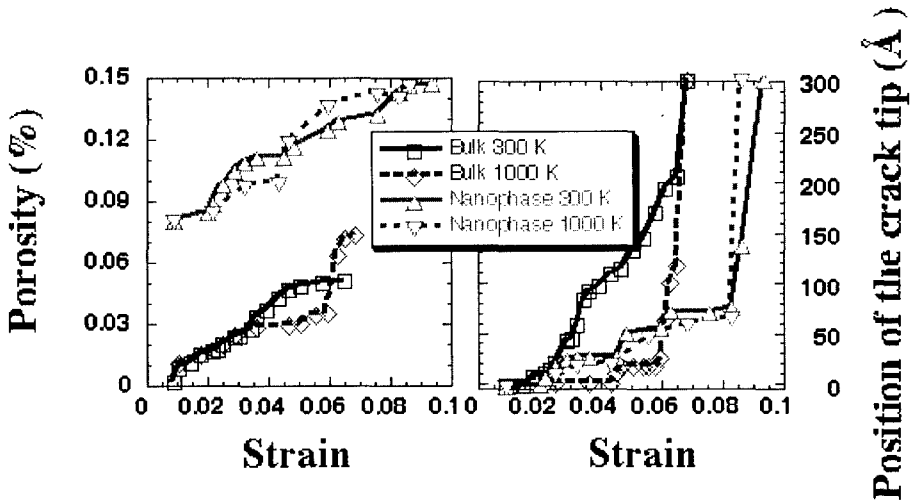

Figure 4. (a) Percentage of porosity as a function of strain. (b) Position of the crack tip as a function of the applied strain.

position of the crack tip in a-SiO_2 at 300 K advances linearly while in others systems it grows intermittently with increasing. The intermittent growth is much more accentuated in the nanostructured systems. The plateaus in Fig. 4(b) reflect the growth of bigger cavities and/or the formation of secondary cracks ahead of the crack tip. This behavior makes difficult to determine precisely the crack tip velocities, although average crack tip speeds can be estimated. In the case of a-SiO_2 at 300 K the crack propagation starts at a strain of 2 % and it advances at a speed of ~800 m/s up to a strain of 6.4 %. This corresponds to half of the Rayleigh wave speed in the material. In the case of a-SiO_2 at 1000 K the crack tip advances at a strain of 4.2 % reaching a plateau within a small increment of strain. The crack tip hardly advances until the strain reaches 6%. Subsequently, the primary crack tip coalesces with the secondary crack. These results strongly indicate that the strain energy in a-SiO_2 at 300 K is dissipated along the crack tip, whereas in a-SiO_2 at 1000 K the strain energy is also dissipated in the formation and growth of pores into secondary crack.

Strained nanostructured silica systems also exhibit alternating plateaus and crack growth. In the nanostructured system at 300 K the onset of crack growth occurs at a strain of 1.5 % followed by a plateau at strains between 3 % and 4.5 %. Further increase in strain results in an other plateau. Finally, at a strain of 8.2 % the system undergoes intergranular fracture. These results provide clear evidence that the strain energy supplied to this system is dissipated via the creation of pores. As a result, this system fracture at a higher strain than its bulk counterparts.

Hence, the augmentation of the temperature in the case of the a-SiO_2 enhances the creation of pores. In the case of the nanostructured the presence of many pores intrinsic of the material plays the same role than the augmentation of the temperature. Therefore, the influence of the temperature in the nanostructured material is smaller than in the bulk.

We have also examined the relationship between structural correlations and crack growth in the bulk and nanostructured a-SiO_2. Experiments and atomic simulations have shown that amorphous silica consists of corner-sharing SiO_4 tetrahedra which form mostly 5-, 6- and 7-membered rings [8]. In so far as the short-range order is concerned, pair-distribution functions and bond-angle distributions do not reveal any notable differences and the corner-sharing tetrahedral structure is mostly unaffected during crack propagation. The influence of

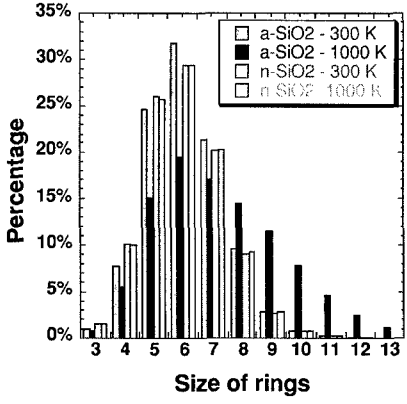

Figure 5. Distribution of the membered rings for the bulk a-SiO_2 and nanophase a-SiO_2 (n-SiO_2) at 1 % of strain corresponding to the strain just before the crack propagation.

intermediate-range order on crack initiation is analyzed through the ring distribution. Figure 5 shows these distributions for the four systems just before the onset of crack propagation. (Rings are identified by a procedure described in [8]). The two bulk systems have significantly different ring distributions: At 300 K, nearly 80% of the rings have 3 to 7 members and only 12% are 8-13 membered rings; at 1000 K, the population of 3- to 7-membered rings drops to 52% while the percentage of 8-13 membered rings increases to 42%. (Note that a 13-membered ring has the same size as a 10 Å pore.) Thus, pores in bulk a-SiO_2 at 1000 K initiate from the breakup of large rings that are distributed uniformly throughout the volume of the systems. In contrast, the nanostructured systems have nearly the same ring distributions indicating that, in both cases, pores in the interfacial regions grow by breaking up all size rings.

CONCLUSIONS

In conclusion, these million-atom MD simulations show that advancing crack-fronts in bulk silica develop multiple branches and pores which coalesce among themselves and also with the crack-front. The strain energy dissipated in creating nanoscale pores causes the system at higher temperature to fracture at a much higher value of strain. In nanostructured silica glasses pores develop mainly in intergranular regions, crack-fronts meander along intercluster boundaries and they coalesce with pores to cause intergranular fracture. In this case temperature has small influence on the onset of crack.

ACKNOWLEDGMENTS

We would like to thank Dr. E. Bouchaud for stimulating discussions and Dr. K. Hideaki for his technical help. This work was supported by U.S. DOE, AFOSR, NSF and Biological Computation and Visualization Center (BCVC). Simulations were performed on the 32-processor PC cluster in the Concurrent Computing Laboratory for Materials Simulations at Louisisana State University.

REFERENCES

1. R. Ochoa, Th. P. Swiler and J. H. Simmons, J. Non-Cryst. Solids **128**, 57 (1991)
2. Th. P. Swiler, T. Varghese and J. H. Simmons, J. Non-Cryst. Solids **181**, 238 (1995)
3. Th. P. Swiler, J. H. Simmons, A. C. Wright, J. Non-Cryst. Solids **182**, 68 (1995)
4. P.Vashishta, R. K. Kalia, and J. P. Rino, Phys.Rev. B **41**,12197 (1990)
5. S. Susman, K. J. Volin, D. L. Gridsditch, J. P. Rino, R. K. Kalia, and P. Vashishta, Phys. Rev. B **43**, 1194 (1991)
6. W. Jin, P. Vashishta, and R. K. Kalia, Phys. Rev. Lett. **69**, 1387 (1992)
7. T. Campbell, R. K. Kalia, A. Nakano, F. Shimojo, K. Tsuruta and P. Vashishta, Phys. Rev. Lett. **82**, 4018 (1999)
8. J. P. Rino, I. Ebbsjo, R. K. Kalia, A. Nakano, P. Vashishta, Phys. Rev. B **47**, 3053 (1993)